Chapter 5

Small-x Behaviour of $xF_3(x, Q^2)$ Structure Function

This chapter is devoted to the determination of Q^2 and x evolutions of $xF_3(x, Q^2)$ structure function in accord with the leading order(LO), next-to-leading order(NLO) and next-next-to-leading order(NNLO) DGLAP evolution equations within the small-x region. The DGLAP equation is solved up to NNLO for $xF_3(x, Q^2)$ structure function using two Regge ansatz as initial input and solutions for both the inputs are compared with the experimental data from CCFR, NuTeV, CDHSW and CHORUS experiments as well as with the recent MSTW parametrization results. A great phenomenological success is achieved in this regards, which signifies the capability of the expressions in describing the small-x behaviour of this non-singlet structure function and their usefulness in determining the structure functions with a reasonable precision.

5.1 Introduction

One of the significant contributions that neutrino-nucleon interaction has towards the understanding of hadron structure is its ability to produce the parity violating term, $xF_3(x, Q^2)$ which receives contributions from the non-singlet part of the co-efficient function and reflects only the valence quark distribution[61]. It is not marred by the presence of the sea quark and gluon densities about which we have very poor information in particular in the small-x region. Therefore, the neutrino-nucleon scattering

as well as $xF_3(x,Q^2)$ structure function are becoming more important theoretically as well as experimentally for the study of different nuclear effects such as shadowing, anti-shadowing, EMC in parton distribution in nuclei etc. Also the study of neutrino interaction provides the understanding of neutrino propagation in matter, whose importance is seen in astrophysics, cosmology and even geology application.

Further, the Gross-Llewellyn Smith(GLS) sum rule[33, 38, 39] associated with the non-singlet $xF_3(x,Q^2)$ structure function measured in neutrino-nucleon $(\nu - N)$ scattering is one of the best observables to investigate Quantum Chromodynamics(QCD) as a theory of strong interaction. As $xF_3(x,Q^2)$ structure function is not marred by the presence of the sea quark and gluon densities about which we have very poor information in particular in the small-x region and higher order QCD calculations are observed to be largely independent of renormalization scheme, the prediction of GLS sum rule is considered as the robust prediction in pQCD. The determination of the GLS sum rule requires knowledge of $xF_3(x,Q^2)$ structure functions over the entire region of $x \in (0;1)$. The experimentally accessible x range for the neutrino DIS is however limited for the available data and therefore one should extrapolate results to $x = 0$ and $x = 1$. The extrapolation to $x \to 0$, where F_3 structure functions grow strongly, is much more important than the extrapolation to $x \to 1$, where structure functions vanish. Again, it is known that maximum contribution (about 90%) to the GLS sum rule come from the small $x(\leq 0.1)$ region. Because of the large contribution to the GLS sum rule from small x, the small x region is particularly important. Therefore this chapter is an attempt to have the small-x behaviour of $xF_3(x,Q^2)$ structure function by means of solving the DGLAP equation using the two Regge ansatz discussed in chapter 3 as the initial input.

The Dokshitzer-Gribov-Lipatov-Altarelli-Parisi (DGLAP) evolution equation [24, 137] which describe the Q^2 behavior of unpolarised non-singlet structure function $xF_3(x,Q^2)$ in perturbative Quantum Chromodynamics (QCD) formalism is given by

$$\frac{\partial xF_3(x,Q^2)}{\partial \ln Q^2} = \int_x^1 \frac{d\omega}{\omega}\frac{x}{\omega}F_3(\frac{x}{\omega},Q^2)P(\omega), \tag{5.1}$$

where, $P(\omega)$ is the splitting function associated with $xF_3(x,Q^2)$ structure function, which is defined up to NNLO by[31]

$$P(\omega) = \frac{\alpha(Q^2)}{2\pi}P^{(0)}(\omega) + \Big(\frac{\alpha(Q^2)}{2\pi}\Big)^2 P^{(1)}(\omega) + \Big(\frac{\alpha(Q^2)}{2\pi}\Big)^3 P^{(2)}(\omega). \tag{5.2}$$

Here, $P^{(0)}(\omega)$, $P^{(1)}(\omega)$ and $P^{(2)}(\omega)$ are the corresponding leading order(LO), next-to-leading order (NLO) and next-next-to-leading order(NNLO) corrections to the splitting functions. These splitting functions are given in Appendices.

Again, in LO, NLO and NNLO, the running coupling constant $\frac{\alpha(Q^2)}{2\pi}$ has the forms[23],

$$\left(\frac{\alpha(t)}{2\pi}\right)_{LO} = \frac{2}{\beta_0 t}, \tag{5.3}$$

$$\left(\frac{\alpha(t)}{2\pi}\right)_{NLO} = \frac{2}{\beta_0 t}\left[1 - \frac{\beta_1 \ln t}{\beta_0^2 t}\right] \tag{5.4}$$

and

$$\left(\frac{\alpha(t)}{2\pi}\right)_{NNLO} = \frac{2}{\beta_0 t}\left[1 - \frac{\beta_1 \ln t}{\beta_0^2 t} + \frac{1}{\beta_0^2 t^2}\left[\left(\frac{\beta_1}{\beta_0}\right)^2 (\ln^2 t - \ln t + 1) + \frac{\beta_2}{\beta_0}\right]\right], \tag{5.5}$$

where $\beta_0 = 11 - \frac{2}{3}N_F$, $\beta_1 = 102 - \frac{38}{3}N_F$ and $\beta_2 = \frac{2857}{6} - \frac{6673}{18}N_F + \frac{325}{54}N_F^2$ are the one-loop, two-loop and three-loop corrections to the QCD β-function. Here the running coupling constant is expressed in terms of the variable t, which is defined by $t = \ln(\frac{Q^2}{\Lambda^2})$.

For simplicity, defining $xF_3(x,Q^2) = F_3^{NS}(x,Q^2)$ and then substituting the respective splitting functions along with the corresponding running coupling constant in (5.1), the DGLAP evolution equations in LO, NLO and NNLO become

$$\frac{\partial F_3^{NS}(x,t)}{\partial t} = \left(\frac{\alpha(t)}{2\pi}\right)_{LO}\left[\frac{2}{3}\{3 + 4ln(1-x)\}F_3^{NS}(x,t) + I_1(x,t)\right], \tag{5.6}$$

$$\frac{\partial F_3^{NS}(x,t)}{\partial t} = \left(\frac{\alpha(t)}{2\pi}\right)_{NLO}\left[\frac{2}{3}\{3 + 4ln(1-x)\}F_3^{NS}(x,t) + I_1(x,t)\right] + \left(\frac{\alpha(t)}{2\pi}\right)^2_{NLO} I_2(x,t), \tag{5.7}$$

and

$$\frac{\partial F_3^{NS}(x,t)}{\partial t} = \left(\frac{\alpha(t)}{2\pi}\right)_{NNLO}\left[\frac{2}{3}\{3 + 4ln(1-x)\}F_3^{NS}(x,t) + I_1(x,t)\right] + \left(\frac{\alpha(t)}{2\pi}\right)^2_{NNLO} I_2(x,t) + \left(\frac{\alpha(t)}{2\pi}\right)^3_{NNLO} I_3(x,t) \tag{5.8}$$

respectively. Here Λ is the QCD cut-off parameter and the integral functions are given by

$$I_1(x,t) = \int_x^1 \frac{d\omega}{1-\omega}\left\{\frac{1+\omega^2}{\omega}F_3^{NS}\left(\frac{x}{\omega},t\right) - 2F_3^{NS}(x,t)\right\}, \tag{5.9}$$

$$I_2(x,t) = \int_x^1 \frac{d\omega}{\omega}P^{(1)}(\omega)F_3^{NS}\left(\frac{x}{\omega},t\right) \tag{5.10}$$

and

$$I_3(x,t) = \int_x^1 \frac{d\omega}{\omega}P^{(2)}(\omega)F_3^{NS}\left(\frac{x}{\omega},t\right). \tag{5.11}$$

The DGLAP equations up to NNLO ((5.6)-(5.8)) can be solved analytically using the ansatz $xF_3(x,t) = A(t)x^{0.5}$ and $xF_3(x,t) = Bx^{(1-at)}$ as the initial inputs and I have discussed bellow in detailed.

5.2 Solution of DGLAP Evolution Equations with the Initial Input $xF_3(x,t) = A(t)x^{0.5}$

On substitution of

$$xF_3(x,t) = F_3^{NS}(x,t) = A(t)x^{0.5} \tag{5.12}$$

and hence

$$xF_3(\frac{x}{\omega},t) = F_3^{NS}(\frac{x}{\omega},t) = A(t)x^{0.5}\omega^{-0.5} = F_3^{NS}(x,t)\omega^{-0.5} \tag{5.13}$$

in the equations (5.6), (5.7) and (5.8) we obtain

$$\frac{\partial F_3^{NS}(x,t)}{\partial t} = \left(\frac{\alpha(t)}{2\pi}\right)_{LO}\left[\frac{2}{3}\{3+4ln(1-x)\} + \frac{4}{3}\int_x^1 \frac{d\omega}{1-\omega}\left\{\frac{1+\omega^2}{\omega}\omega^{-0.5} - 2\right\}\right]F_3^{NS}(x,t), \tag{5.14}$$

$$\frac{\partial F_3^{NS}(x,t)}{\partial t} = \left(\frac{\alpha(t)}{2\pi}\right)_{NLO}\left[\frac{2}{3}\{3+4ln(1-x)\} + \frac{4}{3}\int_x^1 \frac{d\omega}{1-\omega}\left\{\frac{1+\omega^2}{\omega}\omega^{-0.5} - 2\right\}\right]F_3^{NS}(x,t) + \left(\frac{\alpha(t)}{2\pi}\right)^2_{NLO}\int_x^1 \frac{d\omega}{\omega}P^{(1)}(\omega)\omega^{-0.5}F_3^{NS}(x,t) \tag{5.15}$$

and

$$\frac{\partial F_3^{NS}(x,t)}{\partial t} = \left(\frac{\alpha(t)}{2\pi}\right)_{NNLO}\left[\frac{2}{3}\{3+4ln(1-x)\}+\frac{4}{3}\int_x^1\frac{d\omega}{1-\omega}\left\{\frac{1+\omega^2}{\omega}\omega^{-0.5)}-2\right\}\right]F_3^{NS}(x,t)+\left(\frac{\alpha(t)}{2\pi}\right)^2_{NNLO}\int_x^1\frac{d\omega}{\omega}P^{(1)}(\omega)\omega^{-0.5)}F_3^{NS}(x,t)+\left(\frac{\alpha(t)}{2\pi}\right)^3_{NNLO}\int_x^1\frac{d\omega}{\omega}P^{(2)}(\omega)\omega^{-0.5}F_3^{NS}(x,t) \quad (5.16)$$

respectively. These equations can be rearranged to have three ordinary differential equations in terms of $F_3^{NS}(x,t)$,

$$\frac{\partial F_3^{NS}(x,t)}{\partial t} = \frac{\alpha(t)}{2\pi}U(x)F_3^{NS}(x,t), \quad (5.17)$$

$$\frac{\partial F_3^{NS}(x,t)}{\partial t} = \left[\left(\frac{\alpha(t)}{2\pi}\right)_{NLO}U(x)+\left(\frac{\alpha(t)}{2\pi}\right)^2_{NLO}V(x)\right]F_3^{NS}(x,t), \quad (5.18)$$

and

$$\frac{\partial F_3^{NS}(x,t)}{\partial t} = \left[\left(\frac{\alpha(t)}{2\pi}\right)_{NNLO}U(x)+\left(\frac{\alpha(t)}{2\pi}\right)^2_{NNLO}V(x)+\left(\frac{\alpha(t)}{2\pi}\right)^3_{NNLO}W(x)\right]F_3^{NS}(x,t), \quad (5.19)$$

which can be easily solved to have

$$F_3^{NS}(x,t)\Big|_{LO} = C_1\exp\left[U(x)\int\left(\frac{\alpha(t)}{2\pi}\right)_{LO}dt\right], \quad (5.20)$$

$$F_3^{NS}(x,t)\Big|_{NLO} = C_2\exp\left[U(x)\int\left(\frac{\alpha(t)}{2\pi}\right)_{NLO}dt+V(x)\int\left(\frac{\alpha(t)}{2\pi}\right)^2_{NLO}dt\right] \quad (5.21)$$

and

$$F_3^{NS}(x,t)\Big|_{NNLO} = C_3\exp\left[U(x)\int\left(\frac{\alpha(t)}{2\pi}\right)_{NNLO}dt+V(x)\int\left(\frac{\alpha(t)}{2\pi}\right)^2_{NNLO}dt+W(x)\int\left(\frac{\alpha(t)}{2\pi}\right)^3_{NNLO}dt\right] \quad (5.22)$$

respectively. Here,

$$U(x) = \frac{2}{3}\{3 + 4ln(1-x)\} + \frac{4}{3}\int_x^1 \frac{d\omega}{1-\omega}\left\{\frac{1+\omega^2}{\omega}\omega^{-0.5} - 2\right\}, \tag{5.23}$$

$$V(x) = \int_x^1 \frac{d\omega}{\omega} P^{(1)}(\omega)\omega^{-0.5}, \tag{5.24}$$

$$W(x) = \int_x^1 \frac{d\omega}{\omega} P^{(2)}(\omega)\omega^{-0.5}, \tag{5.25}$$

and C_1, C_2, C_3 are the constants originated due to integration .

Now at a fixed value of $x = x_0$, the t dependence of the structure function $F_3^{NS}(x,t)$ in LO is given by

$$F_3^{NS}(x_0,t)\Big|_{LO} = C_1 \exp\left[U(x_0)\int\left(\frac{\alpha(t)}{2\pi}\right)_{LO} dt\right]. \tag{5.26}$$

Again the value of the structure function at $x = x_0$ and $t = t_0$ in accord with (5.26) is

$$F_3^{NS}(x_0,t_0)\Big|_{LO} = C_1 \exp\left[U(x_0)\int\left(\frac{\alpha(t)}{2\pi}\right)_{LO} dt\right]\Bigg|_{t=t_0}. \tag{5.27}$$

Dividing (5.26) by (5.27) and rearranging a bit we obtain the t evolution of $F_3^{NS}(x,t)$ in accord with the LO DGLAP equation with respect to the point $F_3^{NS}(x_0,t_0)$ as

$$F_3^{NS}(x_0,t)\Big|_{LO} = F_3^{NS}(x_0,t_0) \exp\left[U(x_0)\int_{t_0}^{t}\left(\frac{\alpha(t)}{2\pi}\right)_{LO} dt\right]. \tag{5.28}$$

Again in accord with our preassumption (5.12), the t dependence of $F_3^{NS}(x,t)$ at a particular value of $x = x_0$ is given by

$$F_3^{NS}(x_0,t) = A(t)x_0^{0.5}. \tag{5.29}$$

Dividing (5.12) by (5.29), we have the following relation

$$F_3^{NS}(x,t) = F_3^{NS}(x_0,t)\left(\frac{x}{x_0}\right)^{0.5}, \tag{5.30}$$

which describes both t and x dependence of $F_3^{NS}(x,t)$ structure function in terms of the t dependent function $F_3^{NS}(x_0,t)$.

Now combining (5.28) and (5.30) we obtain the relation,

$$F_3^{NS}(x,t)\Big|_{LO} = F_3^{NS}(x_0,t_0)\exp\left[U(x_0)\int_{t_0}^{t}\left(\frac{\alpha(t)}{2\pi}\right)_{LO}dt\right]\left(\frac{x}{x_0}\right)^{0.5}, \tag{5.31}$$

which describes both t and x dependence of $F_3^{NS}(x,t)$ structure function in LO in terms of the input point $F_3^{NS}(x_0,t_0)$.

Proceeding in the similar way we can obtain the expressions representing both x and t dependence of $F_3^{NS}(x,t)$ structure function in terms of an input point $F_3^{NS}(x_0,t_0)$ in NLO and NNLO as

$$F_3^{NS}(x,t)\Big|_{NLO} = F_3^{NS}(x_0,t_0)\exp\left[U(x_0)\int_{t_0}^{t}\left(\frac{\alpha(t)}{2\pi}\right)_{NLO}dt + V(x_0)\int_{t_0}^{t}\left(\frac{\alpha(t)}{2\pi}\right)^2_{NLO}dt\right]\left(\frac{x}{x_0}\right)^{0.5} \tag{5.32}$$

and

$$F_3^{NS}(x,t)\Big|_{NNLO} = F_3^{NS}(x_0,t_0)\exp\left[U(x_0)\int_{t_0}^{t}\left(\frac{\alpha(t)}{2\pi}\right)_{NNLO}dt + V(x_0)\int_{t_0}^{t}\left(\frac{\alpha(t)}{2\pi}\right)^2_{NNLO}dt + W(x_0)\int_{t_0}^{t}\left(\frac{\alpha(t)}{2\pi}\right)^3_{NNLO}dt\right]\left(\frac{x}{x_0}\right)^{0.5} \tag{5.33}$$

respectively.

5.3 Solution of DGLAP Evolution Equations with the Initial Input $xF_3(x,t) = Bx^{(1-bt)}$

Now considering the ansatz, $xF_3(x,t) = Bx^{(1-bt)}$ as the initial input we obtain the DGLAP equations in LO, NLO and NNLO as

$$\frac{\partial F_3^{NS}(x,t)}{\partial t} = \left(\frac{\alpha(t)}{2\pi}\right)_{LO}\left[\frac{2}{3}\{3+4ln(1-x)\}+\frac{4}{3}\int_x^1\frac{d\omega}{1-\omega}\left\{\frac{1+\omega^2}{\omega}\omega^{(bt-1)} - 2\right\}\right]F_3^{NS}(x,t), \tag{5.34}$$

$$\frac{\partial F_3^{NS}(x,t)}{\partial t} = \left(\frac{\alpha(t)}{2\pi}\right)_{NLO}\left[\frac{2}{3}\{3+4ln(1-x)\}+\frac{4}{3}\int_x^1\frac{d\omega}{1-\omega}\left\{\frac{1+\omega^2}{\omega}\omega^{(bt-1)} -2\right\}\right]F_3^{NS}(x,t)+\left(\frac{\alpha(t)}{2\pi}\right)^2_{NLO}\int_x^1\frac{d\omega}{\omega}P^{(1)}(\omega)\omega^{(bt-1)}F_3^{NS}(x,t), \quad (5.35)$$

and

$$\frac{\partial F_3^{NS}(x,t)}{\partial t} = \left(\frac{\alpha(t)}{2\pi}\right)_{NNLO}\left[\frac{2}{3}\{3+4ln(1-x)\}+\frac{4}{3}\int_x^1\frac{d\omega}{1-\omega}\left\{\frac{1+\omega^2}{\omega}\omega^{(bt-1)} -2\right\}\right]F_3^{NS}(x,t)+\left(\frac{\alpha(t)}{2\pi}\right)^2_{NNLO}\int_x^1\frac{d\omega}{\omega}P^{(1)}(\omega)\omega^{(bt-1)}F_3^{NS}(x,t) +\left(\frac{\alpha(t)}{2\pi}\right)^3_{NNLO}\int_x^1\frac{d\omega}{\omega}P^{(2)}(\omega)\omega^{(bt-1)}F_3^{NS}(x,t) \quad (5.36)$$

respectively, which can be easily solved to have

$$F_3^{NS}(x,t)\Big|_{LO} = C_1\exp\left[\int\left(\frac{\alpha(t)}{2\pi}\right)_{LO}U(x,t)dt\right], \quad (5.37)$$

$$F_3^{NS}(x,t)\Big|_{NLO} = C_2\exp\left[\int\left(\frac{\alpha(t)}{2\pi}\right)_{NLO}U(x,t)dt+\int\left(\frac{\alpha(t)}{2\pi}\right)^2_{NLO}V(x,t)dt\right] \quad (5.38)$$

and

$$F_3^{NS}(x,t)\Big|_{NNLO} = C_3\exp\left[\int\left(\frac{\alpha(t)}{2\pi}\right)_{NNLO}U(x,t)dt+\int\left(\frac{\alpha(t)}{2\pi}\right)^2_{NNLO}V(x,t)dt +\int\left(\frac{\alpha(t)}{2\pi}\right)^3_{NNLO}W(x,t)dt\right] \quad (5.39)$$

respectively. Here

$$U(x,t) = \frac{2}{3}\{3+4ln(1-x)\}+\frac{4}{3}\int_x^1\frac{d\omega}{1-\omega}\left\{\frac{1+\omega^2}{\omega}\omega^{(bt-1)}-2\right\}, \quad (5.40)$$

$$V(x,t) = \int_x^1\frac{d\omega}{\omega}P^{(1)}(\omega)\omega^{(bt-1)}, \quad (5.41)$$

$$W(x,t) = \int_x^1 \frac{d\omega}{\omega} P^{(2)}(\omega)\omega^{(bt-1)} \tag{5.42}$$

and C_1, C_2 and C_3 are the constants originated due to integration.

At a fixed value of $x = x_0$, the t dependence of the structure function in LO is given by

$$F_3^{NS}(x_0,t) = C_1 \exp\left[\int \left(\frac{\alpha(t)}{2\pi}\right)_{LO} U(x_0,t)dt\right]. \tag{5.43}$$

Again the value of the structure function at $x = x_0$ and $t = t_0$ in accord with (5.43) is given by

$$F_3^{NS}(x_0,t_0) = C_1 \exp\left[\int \frac{\alpha(t)}{2\pi} U(x_0,t)dt\right]\Bigg|_{t=t_0}. \tag{5.44}$$

Dividing (5.43) by (5.44) and rearranging a bit we obtain the t dependence of $F_3^{NS}(x,t)$ in accord with LO DGLAP evolution equation with respect to the point $F_3^{NS}(x_0,t_0)$ as

$$F_3^{NS}(x_0,t) = F_3^{NS}(x_0,t_0) \exp\left[\int_{t_0}^{t} \left(\frac{\alpha(t)}{2\pi}\right)_{LO} U(x_0,t)dt\right]. \tag{5.45}$$

Again, as both t and x dependence of $F_3^{NS}(x,t)$ is assumed to satisfy

$$F_3^{NS}(x,t) = B.x^{(1-bt)} \tag{5.46}$$

relation, and at any fixed $x = x_0$ we have

$$F_3^{NS}(x_0,t) = B.x_0^{(1-bt)}, \tag{5.47}$$

which represents the t dependence of the structure function at any fixed value of $x = x_0$. Dividing (5.46) by (5.47) we have the following relation

$$F_3^{NS}(x,t) = F_3^{NS}(x_0,t)\left(\frac{x}{x_0}\right)^{(1-bt)}, \tag{5.48}$$

which gives both t and x dependence of $F_3^{NS}(x,t)$ structure function in terms of the t dependent function $F_3^{NS}(x_0,t)$ at fixed $x = x_0$.

Now combining (5.45) and (5.48) we obtain the expression representing both x and t dependence of $F_3^{NS}(x,t)$ structure function in terms of an input point $F_3^{NS}(x_0,t_0)$ in LO as

$$F_3^{NS}(x,t)\Big|_{LO} = F_3^{NS}(x_0,t_0)\exp\left[\int_{t_0}^{t}\left(\frac{\alpha(t)}{2\pi}\right)_{LO} U(x_0,t)dt\right]\left(\frac{x}{x_0}\right)^{(1-bt)}. \tag{5.49}$$

Similarly we may have the joint x and t dependence of $F_3^{NS}(x,t)$ structure function in NLO and NNLO as

$$F_3^{NS}(x,t)\Big|_{NLO} = F_3^{NS}(x_0,t_0)\exp\left[\int_{t_0}^{t}\left(\frac{\alpha(t)}{2\pi}\right)_{NLO} U(x_0,t)dt + \int_{t_0}^{t}\left(\frac{\alpha(t)}{2\pi}\right)^2_{NLO} V(x_0,t)dt\right]\left(\frac{x}{x_0}\right)^{(1-bt)} \tag{5.50}$$

and

$$F_3^{NS}(x,t)\Big|_{NNLO} = F_3^{NS}(x_0,t_0)\exp\left[\int_{t_0}^{t}\left(\frac{\alpha(t)}{2\pi}\right)_{NNLO} U(x_0,t)dt + \int_{t_0}^{t}\left(\frac{\alpha(t)}{2\pi}\right)^2_{NNLO} V(x_0,t)dt + \int_{t_0}^{t}\left(\frac{\alpha(t)}{2\pi}\right)^3_{NNLO} W(x_0,t)dt\right]\left(\frac{x}{x_0}\right)^{(1-bt)}. \tag{5.51}$$

5.4 Results and Discussion

The equations (5.31)-(5.33) and (5.49)-(5.51) are the analytic expressions representing both x and Q^2 dependence of $xF_3(x,Q^2)$ structure function jointly, obtained by means of solving the DGLAP equations in LO, NLO and NNLO incorporating the Regge ansatz, $xF_3(x,Q^2) = A(Q^2)x^{0.5}$ and $xF_3(x,Q^2) = Bx^{1-bt}$ as the initial inputs respectively. These expressions are consisting of an input point $xF_3(x_0,t_0)$, which can be taken from the available experimental data. If the input point is more accurate and precise, we can expect batter results. There are not any specific reason in choosing the input point. Any one of the data points at a certain value of $x = x_0$ and $t = t_0$ can be considered as the input point. Off course, the sensitivity of different inputs

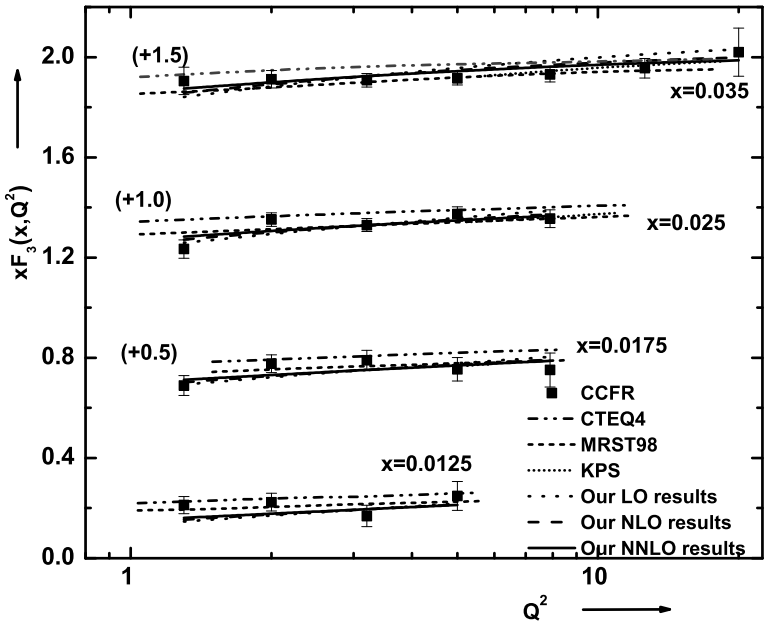

Figure 5.1: Q^2 evolution of $xF_3(x,Q^2)$ structure functions in accord with (5.31)-(5.33). For clarity, the points are offset by the amount given in parenthesis. (Q^2's are taken in the unit of GeV^2).

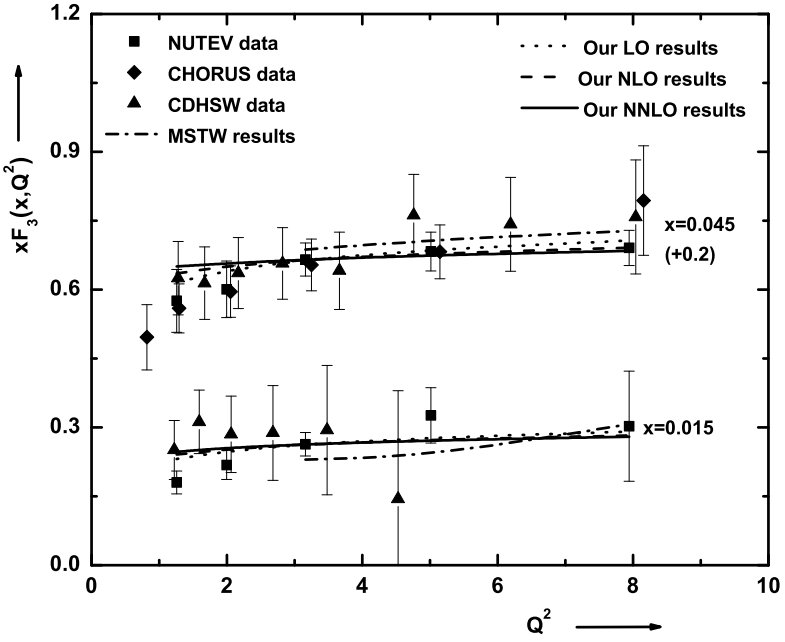

Figure 5.2: Q^2 evolution of $xF_3(x,Q^2)$ structure functions in accord with (5.31)-(5.33). For clarity, the points are offset by the amount given in parenthesis. (Q^2's are taken in the unit of GeV^2).

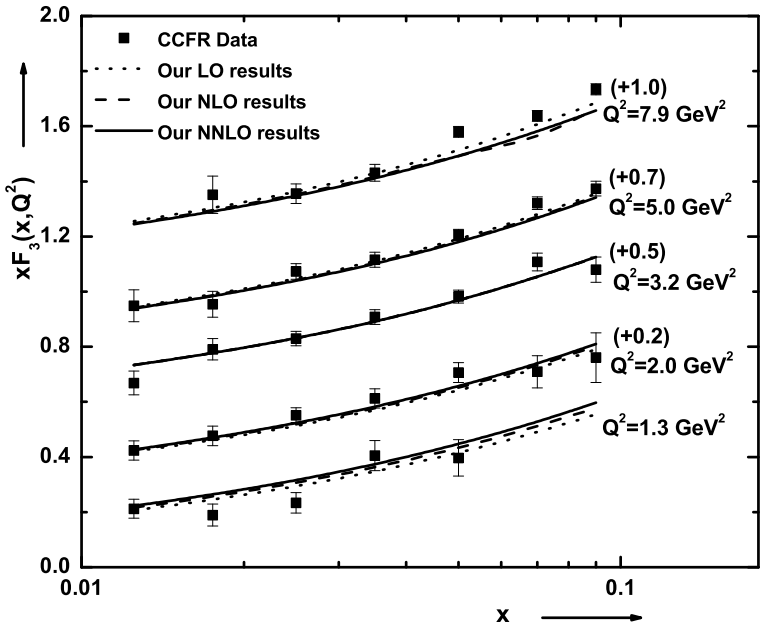

Figure 5.3: x evolution of $xF_3(x,Q^2)$ structure functions in accord with (5.31)-(5.33) in comparison with CCFR[66] data. For clarity, the points are offset by the amount given in parenthesis.

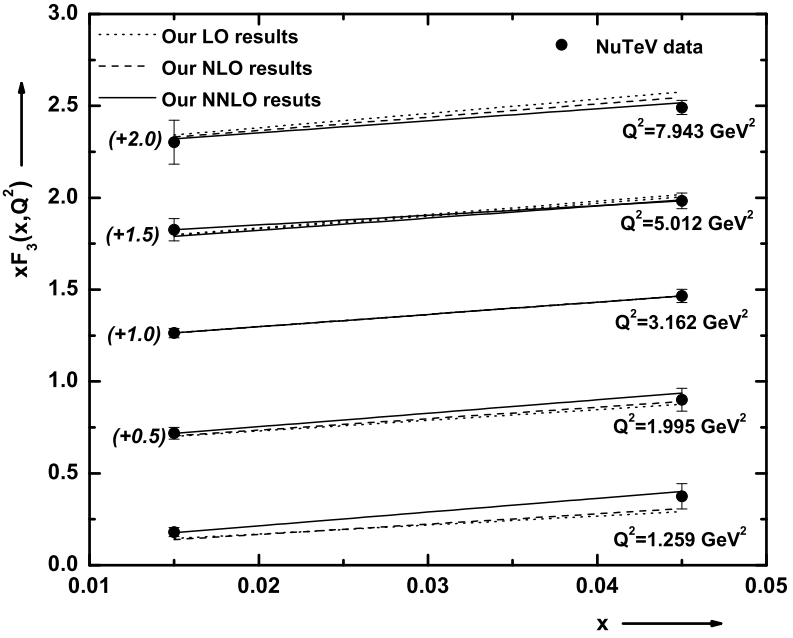

Figure 5.4: x evolution of $xF_3(x,Q^2)$ structure functions in accord with (5.31)-(5.33) in comparison with NuTeV[68] results. For clarity, the points are offset by the amount given in parenthesis.

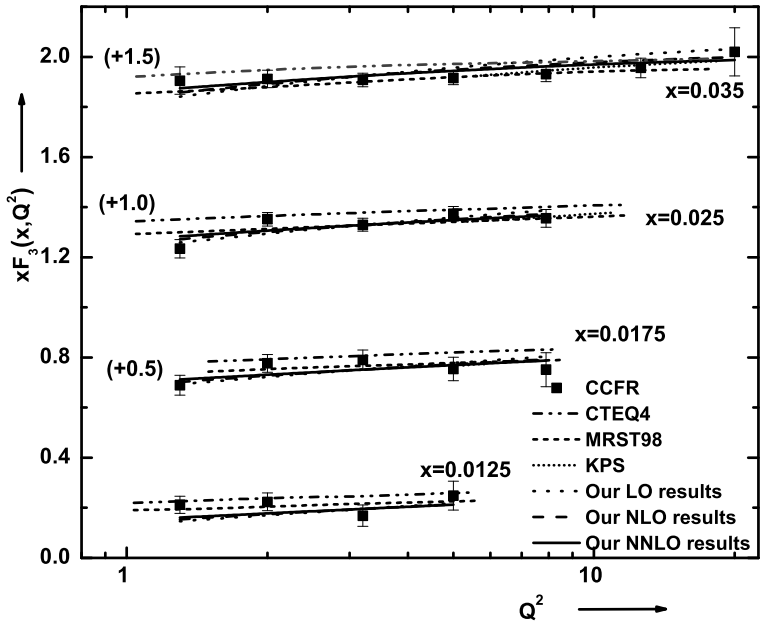

Figure 5.5: Q^2 evolution of $xF_3(x,Q^2)$ structure functions in accord with (5.49)-(5.51) in comparison with CCFR[66] and MSTW[107] results. For clarity, the points are offset by the amount given in parenthesis. (Q^2's are taken in the unit of GeV^2)

will be different. However instead of choosing the input point on the basis of their sensitivity, in our manuscript we have incorporated a suitable condition in determining the input point. We have considered that particular point from the most recent measurements as the input point in which experimental errors are minimum. Under this condition we have selected the point $xF_3(x_0,t_0) = 0.3298$ at $x_0 = 0.025$ and $Q^2 = 3.2GeV^2$ from the experimental results of CCFR[66]. Here we have considered the central value of the input point. Further the expressions (5.49)-(5.51) consists of the additional parameter a which has the value $b = 0.0744 \pm 0.0136$ for $xF_3(x,Q^2)$ as obtained in Chapter 3.

With the input point $xF_3(x_0,t_0)$, substituting the respective expressions in LO, NLO and NNLO for running coupling constant, $\frac{\alpha_s(t)}{2\pi}$ and performing the corresponding integrations, we have obtained both x as well as Q^2 evolution of $xF_3(x,Q^2)$ structure function in accord with the equations (5.31), (5.32) and (5.33) respectively. The Q^2 evolution results at fixed value of x are depicted in Fig. 5.1 and Fig. 5.2 in comparison with the experimental data taken from CCFR[66], NuTeV[68], CDHSW[69], CHORUS[70] collaborations and with the parametrization results of MRST98[138],

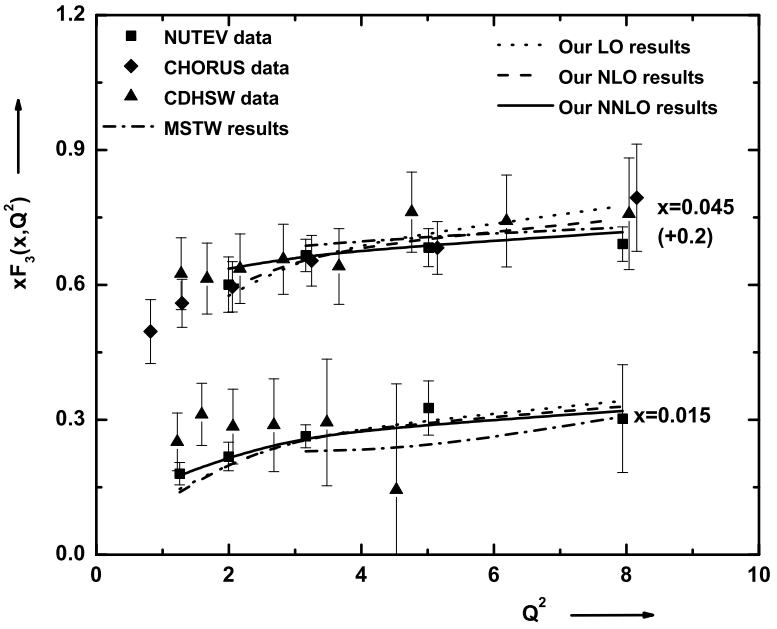

Figure 5.6: Q^2 evolution of $xF_3(x,Q^2)$ structure functions in accord with (5.49)-(5.51) in comparison with NuTeV[68], CHORUS[70], CDHSW[69] and MSTW[107] results. For clarity, the points are offset by the amount given in parenthesis. (Q^2's are taken in the unit of GeV^2)

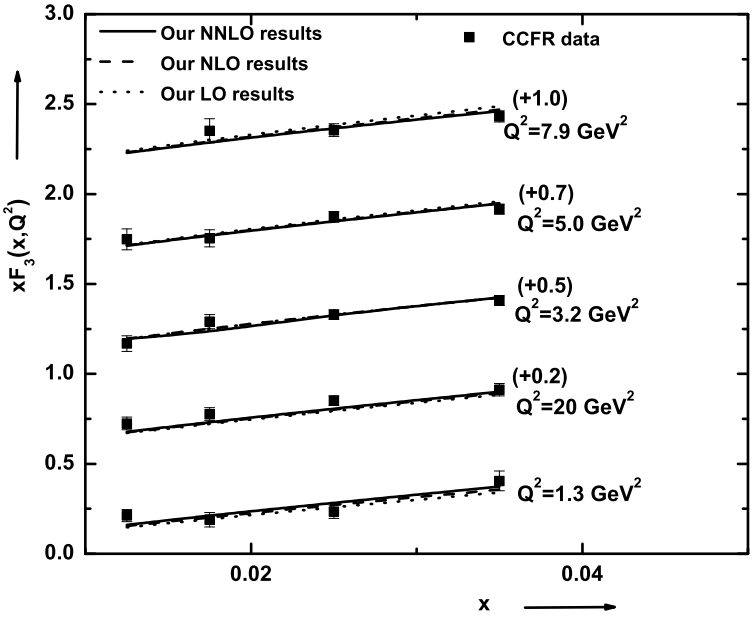

Figure 5.7: x evolution of $xF_3(x,Q^2)$ structure functions in accord with (5.49)-(5.51) in comparison with CCFR[66] and MSTW[107] results. For clarity, the points are offset by the amount given in parenthesis.

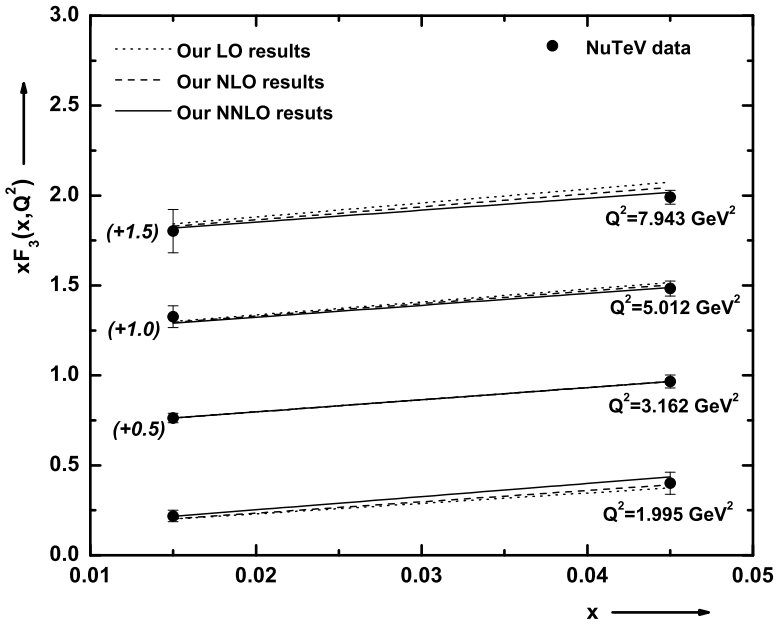

Figure 5.8: x evolution of $xF_3(x,Q^2)$ structure functions in accord with (5.49)-(5.51) in comparison with NuTeV[68], CHORUS[70] and CDHSW[69] results. For clarity, the points are offset by the amount given in parenthesis.

CTEQ4[139], MSTW[107] and KPS[140] results. In Fig. 5.3 and Fig. 5.4, the x evolution of $xF_3(x,Q^2)$ for fixed values of Q^2 are depicted along with CCFR[66], NuTeV[68] results. In all figures, as indicated , the dotted curves represent the LO results, the dashed curves represent NLO results and the solid lines are representing NNLO results. Experimental data are given with vertical upper and lower error bars for total uncertainties of statistical and systematic errors.

Again the results from equations (5.49),(5.50) and (5.51)for Q^2 and x evolution of $xF_3(x,Q^2)$ structure function with $xF_3(x_0,t_0) = 0.3298$ and $b = 0.0744$ are depicted in Fig. 5.5, Fig. 5.6, Fig. 5.7 and Fig. 5.8 respectively. The experimental results from CCFR, NuTeV, CDHSW, CHORUS collaborations and those of MRST98, CTEQ4, MSTW and KPS results are also plotted along with our results. Here, our LO, NLO and NNLO results are represented by the dotted, dashed and solid curves respectively.

As far the figures (Fig. 5.1 - Fig. 5.4) and (Fig. 5.5 - Fig. 5.8) are concerned, we observe a very good consistency between our theoretical and experimental as well as parametrization results within the kinematical region $x < 0.05$ and $Q^2 = 20GeV^2$ of our consideration, especially, if the NNLO results are concerned. The most consistent results, the NNLO results for both the inputs along with other experimental and

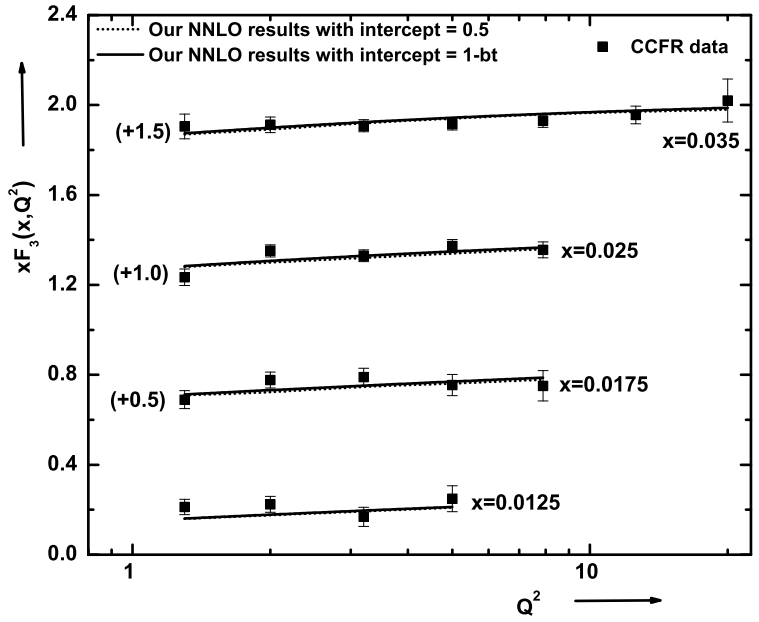

Figure 5.9: Q^2 evolution of $xF_3(x,Q^2)$ structure functions in accord with (5.33) and (5.51) in comparison with CCFR[66] data. For clarity, the points are offset by the amount given in parenthesis. (Q^2's are taken in the unit of GeV^2)

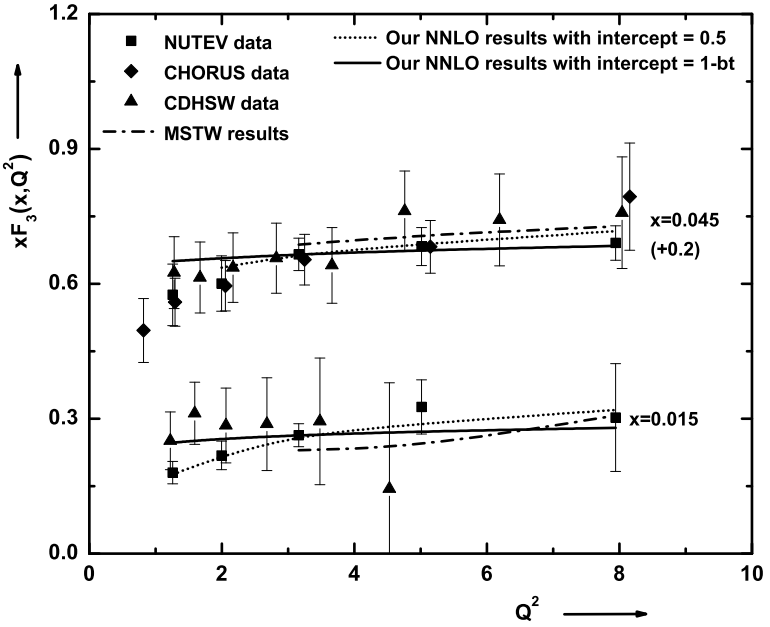

Figure 5.10: Q^2 evolution of $xF_3(x,Q^2)$ structure functions in accord with (5.33) and (5.51) in comparison with NuTeV[68], CHORUS[70], CDHSW[69] and MSTW[107] results. For clarity, the points are offset by the amount given in parenthesis. (Q^2's are taken in the unit of GeV^2)

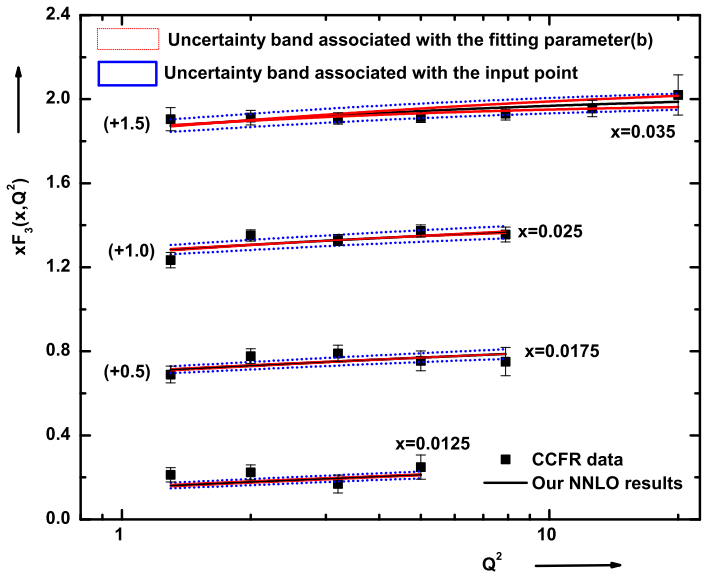

Figure 5.11: NNLO results for $xF_3(x, Q^2)$ structure functions predicted by(5.51) along with the uncertainty band associated with the fitting parameter b and the chosen input point.Our results are compared with CCFR[66] data. For clarity, the points are offset by the amount given in parenthesis.(Q^2's are taken in the unit of GeV^2).

parametrization results are plotted in the figures Fig. 5.9 and Fig. 5.10. They reflect the comparative picture of the results obtained by means of the two ansatz. However within our kinematical region of consideration we do not observe any significant differences among them. Further in Fig. 5.11 our NNLO results predicted by Eq.(5.51) are plotted along with the uncertainty band associated with the fitting parameter and the chosen input point. The uncertainties are observed to be small in both the cases and the uncertainty due to the fitting parameter is considerably less than that of due to input point. Along with the estimated uncertainties, we observe that the Eq.(5.51) has the capability of describing the experimental results with considerable precession.

5.5 Summary

In this chapter the non-singlet structure function $xF_3(x, Q^2)$ has been calculated at small-x. We have employed a unified approach incorporating QCD and Regge theory in this regard. Our results for $xF_3(x, Q^2)$ structure function have been found for two different input to the DGLAP equation. Both the inputs are Regge behaved. One of them consists of constant intercept ($= 0.5$) with Q^2 dependent residue and

the other has Q^2 dependent intercept with constant residue. The structure function, evolved as the solutions of the DGLAP equations are studied phenomenologically in comparison with the results taken from CCFR, NuTeV, CHORUS and CDHSW experimental measurements. In addition, our results are compared with those obtained by MRST98, CTEQ4, MSTW and KPS collaborations. We observe a very good agreement between our theoretical results and other experimental results as well as parametrization, within the kinematical range $x < 0.05$ and $Q^2 = 20GeV^2$ of our consideration. The phenomenological success achieved in this study suggests that the two simple QCD featured Regge behaved ansatz $xF_3(x,Q^2) = A(Q^2)x^{0.5}$ and $xF_3(x,Q^2) = Bx^{1-bt}$ are capable of evolving $xF_3(x,Q^2)$ structure functions with Q^2 in accord with DGLAP equations at small-x. However we could not distinguish the efficiencies among the two models in comparison with experimental data within the kinematical range of our consideration. We hope future experimental measurements at very very small values of Bjorken x will clarify their differences and help us in batter understanding of the structure of nucleon. □□